# Edge Enhancement and Fine Feature Restoration of Segmented Objects using Pyramid Based Adaptive Filtering

A. E. Grace and M. Spann
School of Electronic and Electrical Engineering,
The University of Birmingham,
Edgbaston, Birmingham, United Kingdom B15 2TT.

**Abstract**

A problem often encountered with multiresolution segmentation algorithms is that small or thin features of an object become lost. This is particularly evident in linked-pyramid structures and a method is required to restore these features. This paper shows that simple adaptive isotropic and non-isotropic filtering based on the inter-region signal-to-noise ratio can be used to iteratively re-establish the lost features. It is also shown that boundary placement is also improved and a balance between class certainty and boundary placement is achieved. A number of results are presented for synthetic and real images.

## 1.0. Introduction.

Multiresolution pyramid structures have become a popular platform for segmentation algorithms in recent years [1, 3, 6, 7]. However, one major problem with these structures is that small or thin features become lost due to the smoothing effects of the pyramid structure. Because of this problem a lot of research has tended to consider compact regions and objects only. When objects are not compact, some form of restoration is required after the initial segmentation has taken place. In this paper, an extension to a new algorithm presented in [6] is described that iteratively restores the lost regions even when the inter-region signal-to-noise ratio is low. Further enhancements are described using non-isotropic techniques that establishes the minimum standard deviation from a set of eight possible directions.

## 2.0. Multiresolution structures

The first application of multiresolution data structures to image segmentation problems was discussed in [1, 3]. In these references the idea that a noisy image could be smoothed using a linked-pyramid data structure was introduced. Smoothing methods until this time included local averaging where a pixel becomes the average of itself and its neighbours. This tends to blur edges as a pixel site near a boundary will become the average across the discontinuity. To resolve this, Hong et al. [4] suggest a cooperative process to perform smoothing and segmentation concurrently. The method is based on defining links between different resolutions of the image. At low-resolution versions, region interiors are less noisy. Intuitively, in an image comprising grey scale plus noise, the noise standard deviation will be halved at each lower resolution. The authors point out that the lower the resolution, the less likely it is that a pixel is contained in a single region and that at lower resolutions most pixels will overlap two or more regions.

BMVC 1993 doi:10.5244/C.7.30

The linked-pyramid data structure is a conical set of layers as shown in Figure 1. Each layer has a two-dimension array of nodes which contain properties of the image, such as, average grey-level. At the highest resolution is the image with n x n nodes representing pixel grey-levels. At the lowest resolution there are nodes (up to four) representing regions of the image. If a layer at level m has n x n nodes then a layer at level m-1 (a lower resolution) has n/2 x n/2 nodes. A node in this m-1 layer, called a father, can link to a possible sixteen nodes, called children, in the m layer. A child also has four possible fathers. Therefore, there is an overlapping by 50% in each spatial dimension from layer m-1 to layer m.

Let $L = \{l_s\}$ and $Y = \{y_s\}$ be the set of labels and pixel grey values respectively at pixel site s where $l_s \in \Lambda$ where $\Lambda$ is a finite set of labels and $s \in \Omega$ where $\Omega$ is the image support. The image space comprises k regions where k=1...n and where n=2 in this work. Each node at spatial position (i,j) at level p in the pyramid is defined as v(i,j,p) and the node properties at spatial position (i,j) at pyramid level p are defined as P(v,i,j,p)). In this work these properties are the average grey-scale value but for other image models, such as a quadric model, properties are higher order spatial moments.

A boundary node is one that has one or more of its neighbours as a different class. The boundary nodes of a region with label L at level p defined by the set B(p,L) and those nodes adjacent to boundary nodes B'(p,L). In this work the set of nodes considered for relabelling at a level p is the set of nodes $B(p,L) \cup B'(p,L)$.

The segmentation algorithm iterates between estimating region properties and minimising a log-likelihood function via generation of different pyramid labellings. The algorithm is based around the linked-pyramid data structure. It proceeds in a top-down fashion minimising an error function calculated from the set of moments at the roots of the pyramid. The algorithm starts by setting up the linked-pyramid layers' node values. A node at level n is the quadtree average of a group of nodes at level n+1 [7]. The algorithm starts at the top of the pyramid and raster-scans through each layer. At each node the son-father link is altered if the error is reduced. In this algorithm there is a *stop* layer that is pre-defined. This *stop* layer determines the number of layers involved in the initial segmentation, in other words only a small pyramid is processed initially. When no more son-father links are altered the algorithm proceeds to lower levels. The first small pyramid is then fixed and lower levels are processed in succession until each level converges. When no more links change, an adaptive Gaussian filter is used to improve boundary certainty. The filter is adaptive since it uses the inter-region SNR of the non-boundary sites, that is, where class certainty is high. This process of iterating between linking and filtering continues until the image layer is reached. The class values are then propagated from the root nodes to produce the segmented image. A detailed description of the implementation of the algorithm is given in reference [6] where applications to both grey-scale and texture segmentation are described.

## 3.0. Adapitve node filtering

The algorithm outlined in the previous section produces compact segmentations. However, as the amount of noise present in the image increases then the location of the boundary becomes more uncertain. The aesthetic nature of the boundary can be

improved using an ad-hoc method, for example, a method that minimises the number of boundary nodes will remove small clusters of nodes and generally smooth the boundary. A more intelligent approach is to develop a method dependent on the data that combines the spatial and statistical properties of the pyramid. Thus, the boundary can be improved using a smoothing filter based on the local region properties to generate new node data followed by a re-classification stage.

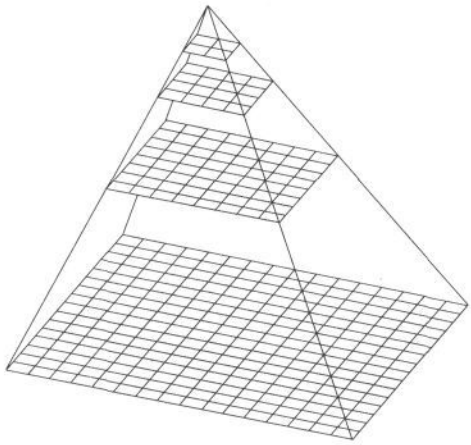

Figure 1. Linked-pyramid structure.

The justification for using such a filtering technique was discussed by Horne [5]. The author states that the segmentation process should be based on spatial and statistical properties and comments that the problem is ill-posed. The filtering process must also be capable of re-introducing small features that have been lost due to the smoothing effect of the multiresolution pyramid. Since the algorithm iterates in a top-down fashion then if an artefact is lost at a higher pyramid level it is impossible to restore it without a filtering stage. For example, if an object comprises two large regions joined by a thin region then they may be segmented as two isolated regions. This suggests an iterative smoothing-re-classification of the set of nodes on or adjacent to the boundary.

Consider a piece-wise flat image containing a single object. If the image is noiseless then it is simple to determine the location of the boundary as it is the discontinuity between the foreground and background. When noise is introduced the exact location of the boundary becomes more difficult to discern.

For the piece-wise flat model an adaptive Gaussian filter was used. It is adaptive in the sense that the width of the Gaussian is determined from the inter-region SNR. For a high inter-region SNR the filter has a sharp profile, the resulting value being dominated by the node value itself. The filter profile is shown in Figure 2. When the inter-region SNR is low and therefore the uncertainty is high the filter profile is broad and the resulting node value is a weighted average of its surrounding neighbours.

The inter-region SNR is defined as

$$\psi = \frac{|u_m - u_n|}{\sqrt{\sigma_m^2 + \sigma_n^2}} \quad \text{where } u_k = \frac{1}{|R_k|}\sum_{s \in R_k} y_s \text{ and where m and n are two region labels.} \qquad (1)$$

and $\sigma_k^2 = \frac{1}{|R_k|}\sum_{s \in R_k}(y_s - u_k)^2$ where $R_k' = \{s : s \in R_k, s \notin (B(p,L) \cup B'(p,L))\}$ is the set of nodes internal to region $R_k$. (2) Let the kernel for a node v(i,j,p) be defined as

$$h_{i,j}(i',j',\psi) = \exp\left(-\frac{1}{2}\frac{r^2}{\sigma^2(\psi)}\right) \qquad \text{where } r = \sqrt{(i-i')^2 + (j-j')^2} \tag{3}$$

The term $\sigma^2(\psi)$ used in [5] was also used here and is given by $\sigma^2(\psi) = 3.0/\psi^2$ (4) This approach is similar to that used by Horne in [5]. The amount of smoothing is limited by the kernel which was set to 5 x 5 and the performance of the filter is such that for $\psi = 0.5$ the smoothing is maximal while for a $\psi = 4.0$ there is no smoothing at all. The procedure for boundary refinement is shown in Figure 3.

The first stage involves convolving the filter defined in Equation 4 with the existing properties of a layer, P(v(i,j,p)) to give new property values P'(v(i,j,p) as

$$P'(v(i,j,p)) = \sum_{i'}\sum_{j'} P(v(i',j',p)) \times h_{i,j}(i',j',\psi)$$ where the summations are over the filter support (5). Nodes are then assigned to the class that is closest in property space. For the two-class case this is if $|P(v(i,j,p)) - u_m| < |P(v(i,j,p)) - u_n|$ then $v(i,j,p) \in R_m$

else $v(i,j,p) \in R_n$ (6)

This two stage procedure iterates until no son-father links change. In this way regions can be grown if small areas have been lost in the segmentation process.

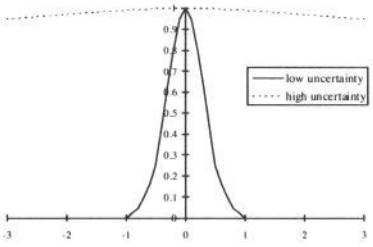


Figure 2. Adaptive filter profile.

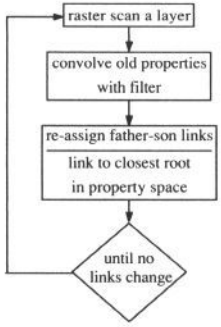


Figure 3. Algorithm for boundary refinement.

The preceding discussion has described an iterative filtering and re-classification process to improve boundary certainty and to grow small regions lost by the inflexibility of the linked-pyramid structure. This occurs when a region that is small becomes detached when the SNR is low and nodes are statistically in the wrong class due to noise. Another cause of lost regions is due to the multiresolution nature of the linked pyramid structure, because lower resolutions of the image, filter the small features in the high resolution version. These regions and features need to be grown and the filter techniques described above are used for this purpose.

## 4.0. Non-isotropic filtering

As discussed earlier, small features are often lost when noise is present. This is due to the smoothing effect of the pyramid and to some extent small regions are re-introduced by the use of the iterative boundary refinement technique discussed in this section. These small regions or thin structures can be improved using directional filters which are required since the isotopic filter used in the boundary technique earlier over-smoothes the thin structures. A suitable technique to overcome this problem is to use a set of directional filters such as those discussed by Dixon [2] where a set of eight directional filters are as shown in Figure 4 for a 5 x 5 mask size. The horizontal filter will provide data that crosses the regions and therefore the standard deviation of the grey-scale data will be high. For the vertical filter, the data will all be from one region and thus the grey-scale data will have a low standard deviation. By selecting the filter that produces the lowest standard deviation, an averaged value for the boundary node can be established which represents a closer approximation to the class model parameters. The node can then be assigned to the class that is closest in distance space.

Referring to Figure 5, the algorithm proceeds as before and after the boundary refinement filtering an iterative-directional filtering algorithm is applied. This finds the direction with the lowest standard deviation and convolves this filter with a one-dimensional Gaussian mask. The class of the node is then established. When this stage has converged, that is, no more son-father links are changed, another isotopic filtering stage with a reduced width Gaussian filter is required to remove isolated pixels to improve the ragged boundary produced by the non-isotropic filtering. The relation between the filter width and the inter-region SNR for the directional filtering is $\sigma^2(\psi) = 5.0 / \psi^2$ and for the isolated pixel removal is $\sigma^2(\psi) = 1.0 / \psi^2$, the relationship for the initial boundary refinement is as before, these being set experimentally [5].

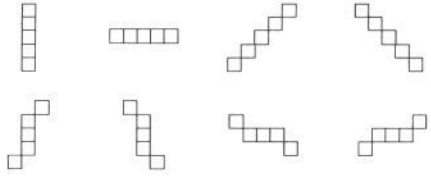

Figure 4. Eight directional filters.

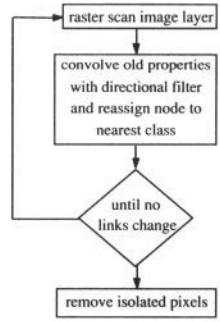


Figure 5. Algorithm for growing thin structures.

## 5.0. Results

The algorithm has been tested with various 128 x 128 x 8 bit images. The first is a synthetic image shown in Figure 6 which has a SNR = 2.0 and Figure 7 which has a SNR = 1.0. In both of these images the problem of uncertainty can be seen and it is difficult to determine the exact boundary location. For these segmentations a pixel error measure can be defined as $E = |C(p,l)| / |B(p,l)|$ (7) where C(p,l) is the set of

misclassified pixels and B(p,l) is the set of boundary nodes which is taken as the object in this case where p is the layer and l is a labelling. Figure 8 shows the resulting segmentations without boundary refinement where at the bottom level and the next level up, the boundary is noisy. When the boundary refinement procedure is applied the resulting boundaries are improved resulting in one compact region as shown in Figure 9, where the pixel/boundary error are shown in Table 1. At higher levels in the pyramid the boundaries are also smoother, indicating that the filtering process has re-assigned some of the father-son links. When the noise is increased to SNR = 1.0 the resulting segmentation has poor boundary definition (see Figure 10). However, it can be seen here that the pyramid has imposed the spatial restrictions. The interior of the region is compact and it is only the boundary area where the uncertainty is high that the segmentation is poor. When the refinement procedure is applied the uncertainty is reduced and the resulting segmentation shows a compact region as shown in Figure 11 and a pixel error is shown in Table 1.

| SNR | without refinement E | with refinementE |
|---|---|---|
| 2.0 | 1.27 | 0.51 |
| 1.0 | 1.31 | 0.66 |

Table 1. Pixel errors for the blob image.

| SNR | without refinement E | with refinementE |
|---|---|---|
| 5.0 | 0.57 | 0.53 |
| 2.5 | 1.03 | 0.53 |
| 1.66 | 1.47 | 0.69 |
| 1.25 | 2.05 | 0.90 |

Table 2. Pixel errors for the valve image.

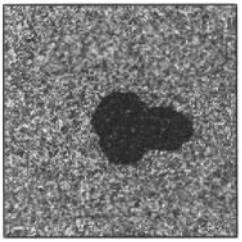

Figure 6. Blob image, SNR = 2.0.

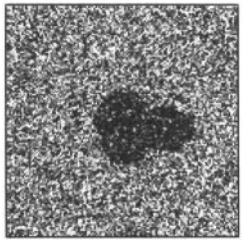

Figure 7. Blob image, SNR = 1.0.

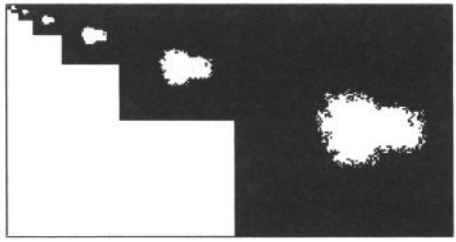

Figure 8 Segmentation of Figure 6, without boundary refinement.

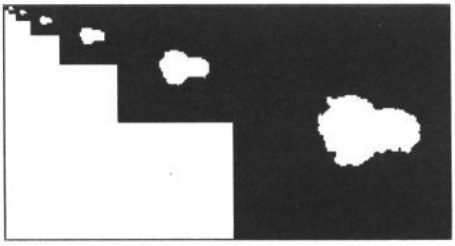

Figure 9. Segmentation of Figure 6, with boundary refinement.

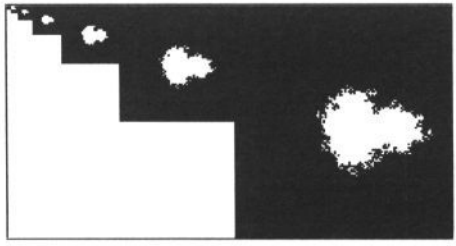

Figure 10. Segmentation of Figure 7, without boundary refinement.

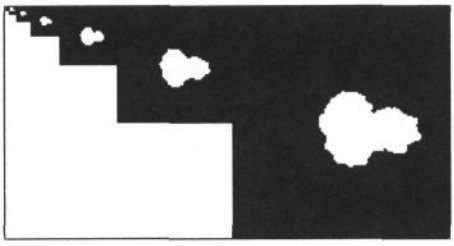

Figure 11. Segmentation of Figure 6, with boundary refinement.

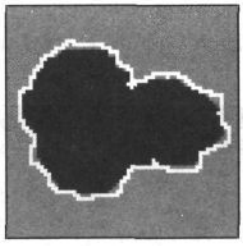

Figure 12. Original Blob image with segmentation overlaid.

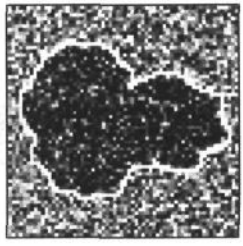

Figure 13. Noisy Blob image with segmentation overlaid.(SNR = 1.0).

Figure 12 shows the segmentation of Figure 11 superimposed onto part of the original image, and a small number of errors can be seen around the boundary. In Figure 13 the same boundary has been superimposed onto the noisy image, illustrating how these errors arise. Where there are errors in the boundary position the grey-levels appear darker, that is, appear to be part of the original object. The segmentation algorithm has performed as desired and without any other knowledge it is impossible to reconstruct the original boundary in high noise.

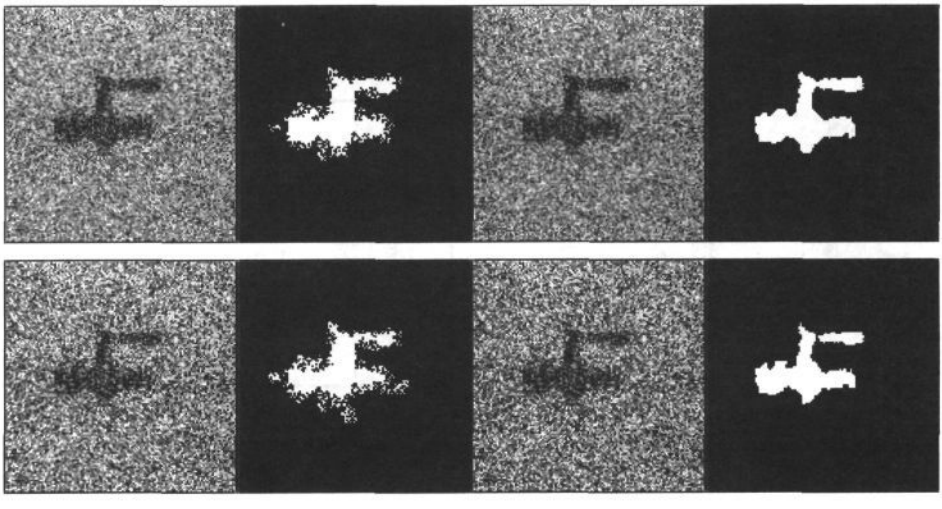

Figure 14. Valve image at various levels of noise with segmentations with and without boundary refinement. From top to bottom the SNR is 1.66 and 1.25.

In Figure 14 an image of a valve is shown with various amounts of added noise up to SNR = 1.0 together with segmentations where, only the bottom layer of the pyramid is shown. This is a more natural image because it is not compact like the previous blob image. The left hand side of this figure shows segmentations without boundary refinement, and as expected the boundaries are not well defined. The right hand side shows segmentations with boundary refinement. Despite not being a compact image the valve tap has been found and it is not until the SNR = 1.0 that the tap becomes detached from the main body. Table 2 shows the boundary/pixel errors and it can be seen that the for the highest amount of noise E = 2.05 in the case of no boundary

refinement. When refinement is used the pixel/boundary error is approximately half at E = 0.90, that is, for each boundary pixel in the original image there is less than one pixel error.

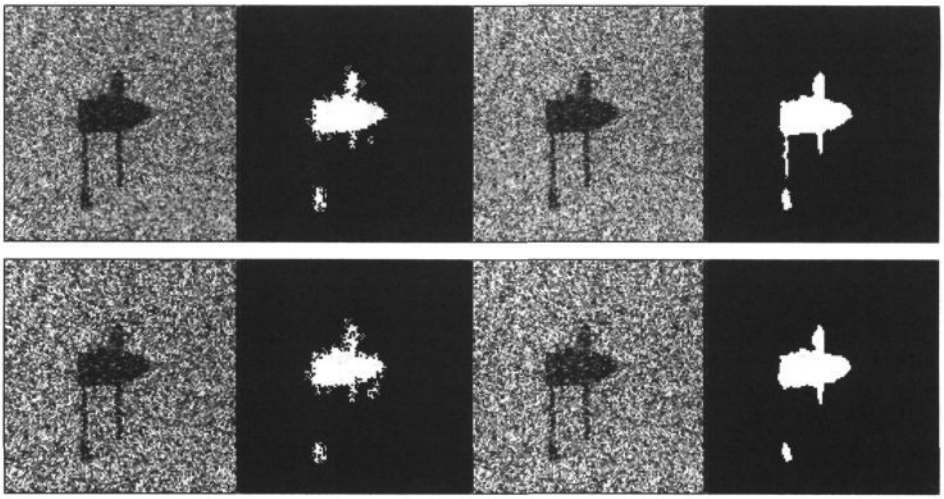

Figure 15. Engineering clamp image at various levels of noise with segmentations with and without boundary refinement. From top to bottom the SNR is 1.66 and 1.25.

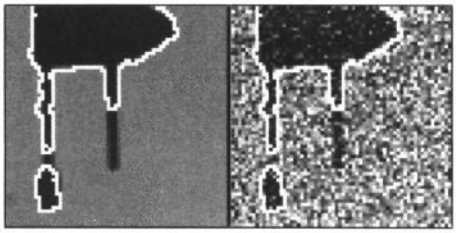

Figure 16. Eng Clamp segmentation overlaid.



Figure 17. Noisy Eng Clamp with with segmentation overlaid

| SNR | without refinement E | with refinement E |
|---|---|---|
| 5.0 | 0.38 | 0.12 |
| 2.5 | 0.61 | 0.20 |
| 1.66 | 0.91 | 0.48 |
| 1.25 | 1.13 | 0.75 |

Table 3. Pixel/boundary errors for the engineering clamp image with and without boundary refinement.

A problem often encountered with multiresolution algorithms is that small or thin parts of an object become lost. In Figure 15, an engineering clamp, the problem is exemplified. The main body of the clamp has two legs protruding from it, one with a finger grip at its end. These legs are only four pixels wide in the image and after two levels of pyramid smoothing the legs are only one pixel wide and at higher levels have been smoothed altogether and cannot be seen. The finger grip is larger and survives to higher levels which can be seen in the top left-hand image. The segmentation has divided the clamp into two regions, however, in the boundary refinement case, the legs have been restored by the region growing nature of the procedure. The boundary/pixel errors can be seen in Table 3 and again, improvement is shown for all levels of added noise. Figures 16 and 17 show part of the engineering clamp image with the

segmentation superimposed onto it. From the figures it can be seen that in the area where the legs are not fully grown the pixel data are corrupted by noise to such an extent that they appear to have become the background. Therefore, without other information it is not possible to establish that these regions should be present.

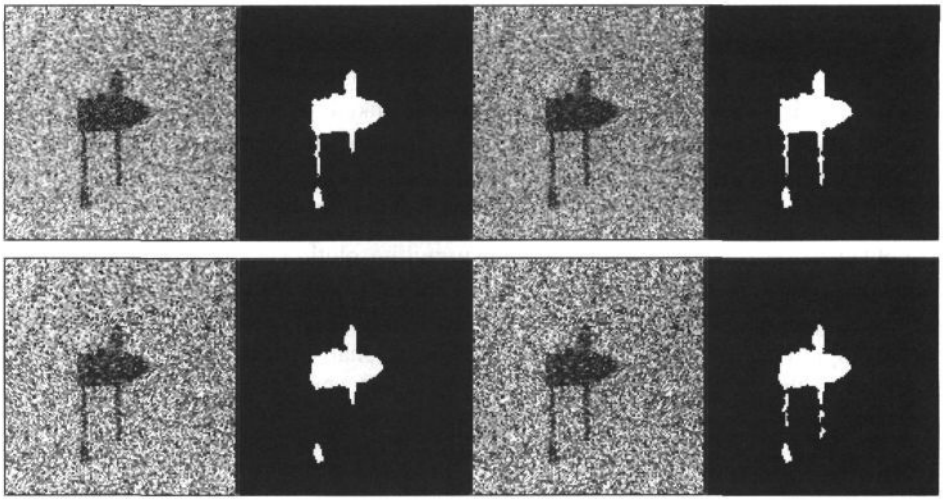

Figure 18. Engineering clamp image at various levels of noise with segmentations with boundary refinement and with directional filtering. From top to bottom the SNR is 1.66 and 1.25.

| SNR | without refinement E | with refinement E |
|---|---|---|
| 5.0 | 0.12 | 0.12 |
| 2.5 | 0.20 | 0.18 |
| 1.66 | 0.48 | 0.38 |
| 1.25 | 0.75 | 0.63 |

Table 4. Pixel errors for the engineering clamp image.

The results of applying the directional filtering algorithm are shown for the engineering clamp in Figure 18. In this figure the segmentations in the second column are the result of the boundary refinement technique and are shown here for comparison. When the SNR is high, the results are no better than the previous method. However, at SNR=1.66 or lower the right hand leg is not segmented. Using the directional technique improves the segmentation although the legs are still not totally connected. Table 4 shows the pixel/boundary errors and some improvement can be seen at low SNRs. It should be noted that these segmentations are a more faithful representation to the image data and that without further assumptions or information (for example, that all regions should be connected) it is not possible to produce connected segmentations from the data.

## 6.0. Conclusions

Boundary uncertainty has been improved for high uncertainty images using an adaptive filtering method which also re-introduces small features that have been lost due to the multiresolution nature of the pyramid. A non-isotropic method was also shown that improved the quality of thin structures when the added noise was high.

It has been shown that boundary uncertainty can be improved using a Gaussian filter, the width of which is dependent on the local inter-region SNR. After the re-linking has converged at a level each node is filtered and linked to the father that is closest in distance space. This process iterates until no more links are changed. Some examples of how this method works have been shown and good boundary placement is established with a balance between class certainty and boundary uncertainty achieved.

A problem often encountered with top-down multiresolution segmentation algorithms is that small or thin features tend to be lost. This has been resolved to some extent by the growing nature of the filtering process that tends to re-introduce lost features. A non-isotropic filtering technique that re-introduces small or thin features. Numerous examples of this method have been shown including comparisons with the isotropic technique.

## Acknowledgements

The Science and Engineering Research Council (UK) and Inmos Ltd. are gratefully thanked for sponsoring this work.

## References

1 Burt, P. J., Hong, T. and Rosenfeld, A., "Segmentation and estimation of image region properties through cooperative hierarchical computation", IEEE Transactions on Systems, Man and Cybernetics, volume SMC-11, number 12, December 1981.

2 Dixon, R. N., "Aspects of picture processing", Ph.D. thesis, University of Manchester, Chapter 7, "A local operator for line segmentation", 1980.

3 Grace, A. E. and Spann, M., "Model based image segmentation using optimisation networks", Proceedings of the 2nd International Conference on Image Processing, Singapore, pages 716-720, 1992.

4 Hong, T., Narayanan, K. A., Peleg, S., Rosenfeld, A. and Silberberg, T., "Image smoothing and segmentation by pixel linking: further experiments and extensions", IEEE Transactions on Systems, Man and Cybernetics, volume SMC-12, number 5, September/October 1982.

5 Horne, C., "Unsupervised image segmentation", Ph.D. thesis, number 805, Ecole Polytechnique, Federale de Lausanne, 1990.

6 Spann, M. and Grace, A. E., "Adaptive segmentation of noisy and textured images", submitted to IEEE Transactions on Pattern Analysis and Machine Intelligence, January 1993.

7 Spann, M. and Wilson, R., "A quad-tree approach to image segmentation which combines statistical and spatial information", Pattern Recognition, volume 18, number 3/4, pages 257-269, 1985.